Temperature susceptibility of a mesophilic anaerobic membrane bioreactor treating saline phenol-containing wastewater

Muñoz Sierra, Julian D.; Wang, Wei; Cerqueda-Garcia, Daniel; Oosterkamp, Margreet J.; Spanjers, Henri; van Lier, Jules B.

Important note
To cite this publication, please use the final published version (if applicable).
Please check the document version above.

Temperature susceptibility of a mesophilic anaerobic membrane bioreactor treating saline phenol-containing wastewater

Julian D. Muñoz Sierra [a, *], Wei Wang [a, b], Daniel Cerqueda-Garcia [a, c], Margreet J. Oosterkamp [a], Henri Spanjers [a], Jules B. van Lier [a]

[a] Section Sanitary Engineering, Department of Water Management, Delft University of Technology, Stevinweg 1, 2628CN, Delft, the Netherlands
[b] Department of Municipal Engineering, School of Civil and Hydraulic Engineering, Hefei University of Technology, Hefei, 230009, China
[c] Institute of Ecology, National Autonomous University of Mexico. Circuito ext. Sn, Cd. Universitaria, Mexico City, Mexico

HIGHLIGHTS

- Phenol degradation was less susceptible to temperature shifts than methanogenesis.
- Phenol conversion rate dropped from 3.16 at 35 °C to 1.69 mgPh·gVSS^{-1}·d^{-1} at 55 °C.
- Biomass properties and microbial community structure in the AnMBR were determined.
- Membrane filtration was negatively impacted with 77% particle size reduction.
- 11 OTUs reported in aromatic degradation showed temperature differential abundance.

GRAPHICAL ABSTRACT
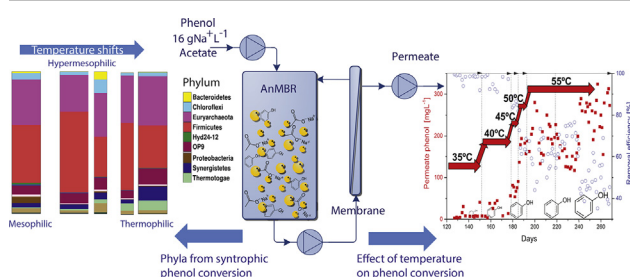
ABSTRACT

This study examined the temperature susceptibility of a continuous-flow lab-scale anaerobic membrane bioreactor (AnMBR) to temperature shifts from 35 °C to 55 °C and its bioconversion robustness treating synthetic phenolic wastewater at 16 gNa$^+$·L^{-1}. During the experiment, the mesophilic reactor was subjected to stepwise temperature increases by 5 °C. The phenol conversion rates of the AnMBR decreased from 3.16 at 35 °C to 2.10 mgPh·gVSS^{-1}·d^{-1} at 45 °C, and further decreased to 1.63 mgPh·gVSS^{-1}·d^{-1} at 50 °C. At 55 °C, phenol conversion rate stabilized at 1.53 mgPh·gVSS^{-1}·d^{-1} whereas COD removal efficiency was 38% compared to 95.5% at 45 °C and 99.8% at 35 °C. Interestingly, it was found that the phenol degradation process was less susceptible for the upward temperature shifts than the methanogenic process. The temperature increase implied twenty-one operational taxonomic units from the reactor's microbial community with significant differential abundance between mesophilic and thermophilic operation, and eleven of them are known to be involved in aromatic compounds degradation. Reaching the upper-temperature limits for mesophilic operation was associated with the decrease in microbial abundance of the phyla Firmicutes and Proteobacteria, which are linked to syntrophic phenol degradation. It was also found that the particle size decreased from 89.4 μm at 35 °C to 21.0 μm at 55 °C. The accumulation of small particles and higher content of soluble microbial protein-like substances led to increased transmembrane pressure which negatively affected the filtration performance. Our findings

* Corresponding author. Present address: KWR Watercycle Research Institute, Groningenhaven 7, 3430BB, Nieuwegein, the Netherlands.
  E-mail address: J.D.MunozSierra@tudelft.nl (J.D. Muñoz Sierra).

indicated that at high salinity a mesophilic AnMBR can tolerate a temperature up to 45 °C without being limited in the phenol conversion capacity.

1. Introduction

Phenolic compounds are toxic organics widely present in industrial wastewater streams such as those coming from coal gasification, coke, pulp-paper manufacturing, and oil-refining (Wang et al., 2017a, 2017c). Anaerobic processes are considered a more sustainable and economically attractive technology for the treatment and mineralization of these compounds (Ramakrishnan and Gupta, 2006). In the past decade, different anaerobic technologies such as the up-flow anaerobic sludge blanket (UASB), anaerobic sequencing batch reactor (AnSBR), anaerobic fluidized bed reactor (AFBR), anaerobic hybrid reactors (AHR) and recently anaerobic membrane bioreactors (AnMBR) were applied to treat wastewaters containing phenolic compounds under mesophilic conditions (Wang et al., 2011a; Ramakrishnan and Surampalli, 2013; Rosenkranz et al., 2013; De Amorim et al., 2015; Muñoz Sierra et al., 2018). Wang et al. (2011a) evaluated a two continuous UASB system for treating coal gasification wastewater at 37 °C obtaining maximum COD and total phenols removal of 55–60% and 58–63% respectively. Rosenkranz et al. (2013) obtained high phenol conversion rate up to 0.8 $gPh \cdot L^{-1}$ in the synthetic phenol-containing wastewater by a mesophilic AnSBR system. Similarly, De Amorim et al. (2015) evaluated a AFBR system and achieved phenol and COD removal efficiencies higher than 91%. Muñoz Sierra et al. (2018) presented the performance robustness of a mesophilic AnMBR under long-term high salinity exposure achieving phenol conversion rates up to 11.7 $mgPh.gVSS^{-1}.d^{-1}$. Interestingly, Ramakrishnan and Surampalli (2013) indicated that with AHR systems the mesophilic anaerobic digestion treating coal wastewater exhibited lower phenolic and COD degradation than thermophilic. Although anaerobic systems exhibited high removal of phenol during stable operation, the fluctuations in phenol concentration and moving to a higher operational temperature were identified as the major obstacles for achieving performance robustness (Levén et al., 2012; Wang and Han, 2012). Earlier research indicated that thermophilic anaerobic digestion in continuous flow reactors could improve the biodegradation rates of phenolic compounds, methane yields, and the aerobic post-treatment when compared to mesophilic (Wang et al., 2011b; Ramakrishnan and Surampalli, 2013). In contrast, Fang et al. (2006) showed that phenol degradation rate at 55 °C was substantially lower than under mesophilic conditions in a UASB reactor with an organic loading rate (OLR) of 0.9 $gCOD \cdot L^{-1} \cdot d^{-1}$ and an influent phenol concentration of 0.63 $gPh \cdot L^{-1}$. Thus far, only a few studies have been done on continuous flow reactors comparing thermophilic and mesophilic phenol degradation even though most of the chemical waste streams appear to have high temperatures. Moreover, due to the need of closing water loops in industry, these wastewaters are becoming more prone to be saline, adding another harsh condition for the anaerobic degradation of the organics (Muñoz Sierra et al., 2017).

Proper (auto-)immobilization of anaerobic biomass is the main challenge in treating industrial wastewater at both high temperatures and high salinity. Poor settling characteristics and dispersed biomass make it challenging to accomplish immobilization in comparison with mesophilic conditions (Dereli et al., 2012). AnMBRs under thermophilic conditions has been recently shown to be a promising technology with different wastewaters (Duncan et al., 2017). Simultaneous occurrence of toxicity, high salinity, and thermophilic conditions increase the need to combine membrane separation with anaerobic treatment to prevent biomass washout, achieve a high-quality effluent and potentially better performance robustness (Lin et al., 2013). Therefore, AnMBRs are considered an appealing alternative for phenolic wastewater treatment under high temperatures and saline conditions, but there are still difficulties to overcome (Jeison and van Lier, 2007; van Lier et al., 2015). Assessment of the bioprocess temperature susceptibility is of particular importance for those reactors that treat wastewaters, which are generated at high temperatures in a wide range, and which require cooling to mesophilic conditions. Boušková et al. (2005) proposed a stepwise shift from 35 °C to 55 °C as a strategy to determine the performance robustness with increasing temperature of a mesophilic anaerobic continuous stirred tank (CSTR) reactor treating sewage sludge. In AnMBR systems, the low concentrated suspended methanogenic sludge is likely more susceptible to such temperature changes, owing to the fact that the biomass activity is less determined by mass transfer limitation. To our knowledge, the application of AnMBRs for saline phenolic chemical wastewater have not been reported, neither the temperature susceptibility of the phenol degradation process linked to microbial community structure analysis. Therefore, the present study aimed to evaluate the temperature susceptibility of a mesophilic AnMBR treating phenol-containing wastewater under high salinity (16 $gNa^+ \cdot L^{-1}$) conditions over the temperature range of 35–55 °C, with focus on process performance as well as microbial community dynamics. To provide better insight into high-temperature exposure, a long-term thermophilic operation was also carried out. The effects of stepwise temperature shifts of 5 °C on biomass properties such as particle size, filterability, and membrane filtration performance were analyzed. Correspondingly, the phenol conversion rates, methanogenic activities and microbial community structure at the different short- and long-term temperature exposure were compared. Particular attention was given to the phenol degrading related operational taxonomic units (OTUs) and their main changes induced by the temperature shift from mesophilic to thermophilic conditions.

2. Material and methods

2.1. Reactor configuration and operation

The experiments were performed using a laboratory scale AnMBR reactor with an effective volume of 6.5 L, equipped with an ultra-filtration (UF) side-stream membrane module. A tubular PVDF membrane (Pentair, The Netherlands) with 5.2 mm inner diameter, 30 nm pore size, and 0.64 m length was used. The system was equipped with feed, recycle and effluent pumps (Watson-Marlow 120U/DV, 220Du), pH and temperature sensors (Endress & Hauser, Memosens), and a biogas meter (Ritter, Milligas Counter MGC-1 PMMA, Germany). Transmembrane pressure (TMP) was measured using three pressure sensors (AE Sensors ATM, The Netherlands). The temperature of the jacketed reactor was controlled by a thermostatic water bath (Tamson Instruments, The Netherlands). The experimental set-up was controlled by a

computer running LabView software (version 15.0.1f1, National Instruments, USA).

The reactor was initially operated under mesophilic conditions ($35.0 \pm 0.8\,°C$) for 152 days. During this time, the influent phenol concentration was gradually increased from 100 to 500 mgPh·L^{-1}. Hereafter, the temperature shift was carried out by stepwise increases of 5 °C up to 55 °C from days 152—193. Subsequently, the reactor was operated until day 270 under thermophilic ($55.0 \pm 0.8\,°C$) conditions (see Fig. 1.). The reactor was fed (0.7 L d^{-1}) with synthetic phenol-containing wastewater with phenol and sodium concentration of 500 mgPh·L^{-1} and 16 gNa$^+$·L^{-1}, respectively. The organic loading rate (OLR) applied was initially 4.35 gCOD·L^{-1}·d^{-1}, however, due to deteriorating process performance,

it was decreased to 1.86 gCOD·L^{-1}·d^{-1} on day 218. An average sludge retention time (SRT) of 43 days was maintained, resulting from biomass growth and biomass sampling.

2.2. Inoculum and model wastewater composition

The reactor was inoculated with mesophilic anaerobic biomass obtained from a full-scale UASB reactor (Shell, Moerdijk, The Netherlands) to be subjected to higher temperatures. The initial concentration of volatile suspended solids (VSS) and total suspended solids (TSS) were 20.1 g·L^{-1} and 50.9 g·L^{-1}, respectively. The model synthetic wastewater consisted of C_6H_6O (0.5 g·L^{-1}), $C_2H_3NaO_2$ (18.2 g·L^{-1}), NaCl (32 g·L^{-1}), yeast extract (0.5 g L^{-1}),
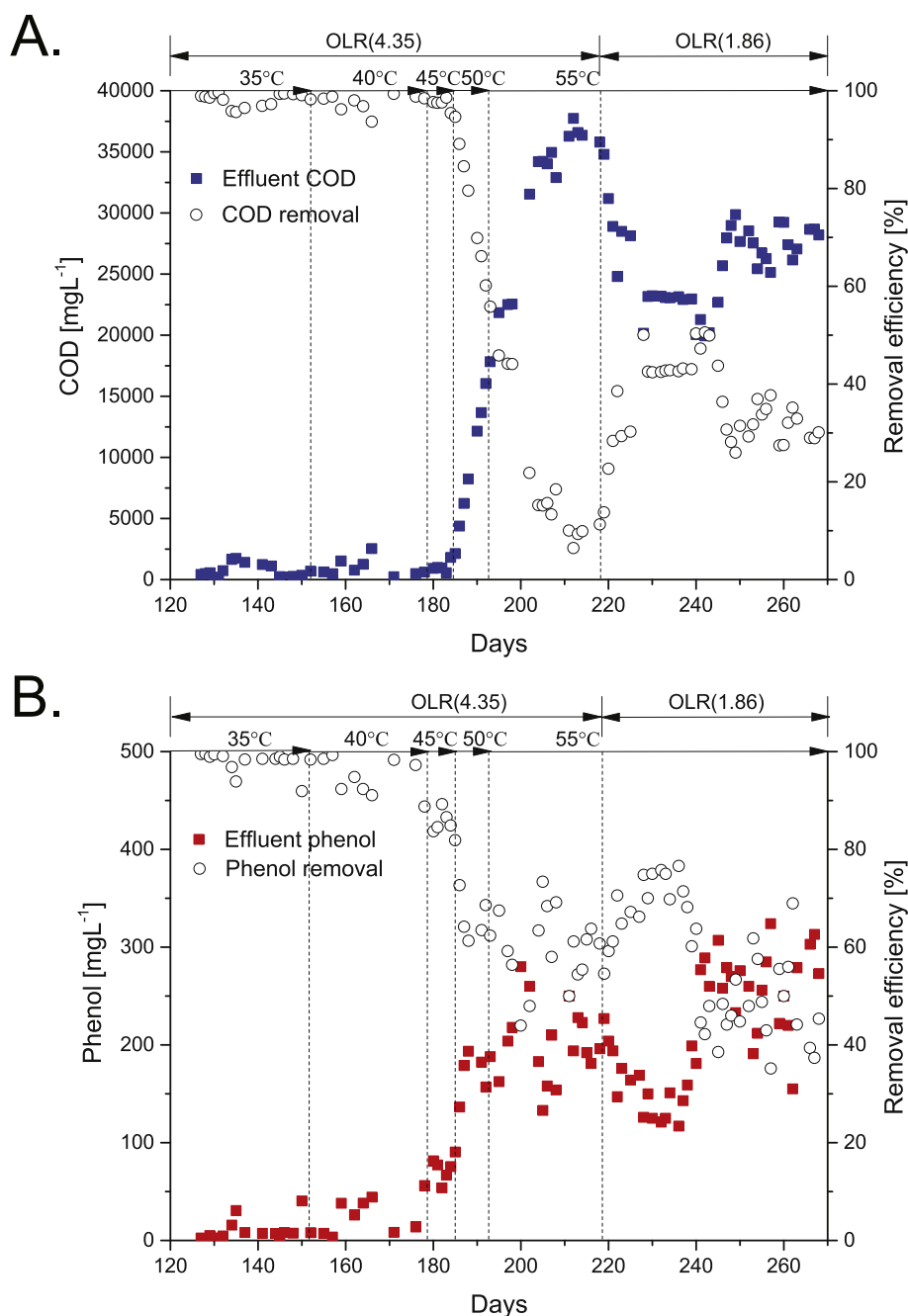

Fig. 1. AnMBR performance under mesophilic, hyper-mesophilic and thermophilic conditions at 16 gNa$^+$·L^{-1}. A. COD removal. B. Phenol removal.

K_2HPO_4 (1.81 g·L^{-1}), NaH_2PO_4 (0.48 g·L^{-1}). Macronutrients (9 mL·L^{-1}), and micronutrients (4.5 mL L^{-1}) solutions were added. Macronutrients solution included (in g·L^{-1}): NH_4Cl (170), $CaCl_2 \cdot 2H_2O$ (8), and $MgSO_4 \cdot 7H_2O$ (9); micronutrients solution contained (in g L^{-1}): $FeCl_3 \cdot 6H_2O$ (2), $CoCl_2 \cdot 6H_2O$ (2), $MnCl_2 \cdot 4H_2O$ (0.5), $CuCl_2 \cdot 2H_2O$ (0.03), $ZnCl_2$ (0.05), H_3BO_3 (0.05), $(NH_4)_6Mo_7O_2 \cdot 4H_2O$ (0.09), Na_2SeO_3 (0.1), $NiCl_2 \cdot 6H_2O$ (0.05), EDTA (1), Na_2WO_4 (0.08). The chemical reagents were of analytical grade. The feed solution pH was adjusted to 7.0−7.5 by using HCl (35%).

2.3. Biomass properties

2.3.1. Extracellular polymeric substances (EPS) and soluble microbial products (SMP)

EPS and SMP were characterized based on proteins and polysaccharides and its Fourier spectrum. Biomass samples were centrifuged at 4 °C and 12000 rpm for 15 min. The supernatant was filtered (0.45 μm) and directly used to measure the SMP as proteins and polysaccharides. EPS extraction was carried out by cation exchange resin method as proposed by Frølund et al. (1996). DOWEX Marathon C (20−50 μm mesh, sodium form, Fluka 91973) was used as cation exchange resin. Extraction was carried out at 4 °C, 800 rpm during 4 h. For the analysis of proteins, the modified Lowry method of Frølund et al. (1996) was applied. Polysaccharides were analyzed following the phenol-sulfuric acid method (Dubois et al., 1956). EPS was normalized against the VSS concentration of the biomass in the reactor.

The functional groups of EPS extracted at different temperatures were characterized with a Fourier Transform Infrared (FT-IR) Spectrometer (Spectrum 100 Series Perkin−Elmer, UK) equipped with a universal Attenuated Total Reflexion (ATR) unit. The spectra were recorded in the range of 4000−550 cm^{-1} with 2 cm^{-1} resolution. The FT-IR was first calibrated for background signal scanning, and then the experimental sample scanning was conducted in triplicate.

2.3.2. Particle size distribution (PSD)

Measurement of PSD was carried out by using a DIPA-2000 EyeTech™ particle analyzer (Donner Technologies, Or Akiva, Israel) with an A100 and B100 laser lens (measuring range 0.1−300 μm and 1−2000 μm, respectively) and a liquid flow cell DCM-104A (10 × 10 mm).

2.3.3. Biomass filterability: capillary suction time (CST) and specific resistance to filtration (SRF)

CST of the biomass was measured by a Capillary Suction Timer device (Model 304M, Triton Electronics, Essex, England, UK). A CST paper (7 × 9 cm) was used for each sample of 6.4 mL of biomass. Samples were measured in triplicate. The results were normalized by TSS concentration. Biomass SRF was measured in a dead-end filtration cell under a 1 bar constant pressure. Permeate production was measured by an electronic balance for data acquisition. SRF was assessed by plotting filtration time/filtrate volume (t/V) versus the filtrate volume (V) and using $SRF = 2\Delta P A^2 b / \mu C$, where ΔP: Pressure (Pa), A: Effective filtration area (m^2), b: Slope of t/V-V plot (s L^{-2}), μ: Viscosity (Pa s), C: TSS concentration (kg m^{-3}) (Dereli et al., 2015b).

2.4. Specific methanogenic activity (SMA) and biogas content

SMA tests were performed in triplicate using an automated methane potential test system (AMPTS, Bioprocess Control, Sweden). All the SMA tests were carried out at 35 °C following the manufacturer's procedure. The pH of all bottles was adjusted to 7.0 (20 ± 0.4 °C). Methane content of the biogas was analyzed using a gas chromatograph 7890A (GC) system (Agilent Technologies, US) equipped with a flame ionization detector.

2.5. Permeate characterization

Hach Lange kits were used to measure chemical oxygen demand (COD). The COD was measured using a VIS - spectrophotometer (DR3900, Hach Lange, Germany) making proper dilutions preventing a negative impact of high chloride concentrations, without compromising the accuracy of the measurement. Phenol was measured by Merck − Spectroquant® Phenol cell kits using a spectrophotometer NOVA60 (Merck, Germany). Phenol concentrations were double-checked using high-pressure liquid chromatography HPLC LC-20AT (Shimadzu, Japan) equipped with a 4.6 mm reversed phase C18 column (Phenomenex, The Netherlands) and a UV detector at a wavelength of 280 nm. The mobile phase used was 25% (v/v) acetonitrile at a flow rate of 0.95 mL min^{-1}. The column oven was set at 30 °C.

2.6. Microbial community structure analysis

Biomass samples were taken every time before the temperature was raised. DNA extraction was performed by using the DNeasy UltraClean Microbial kit (Qiagen, Hilden, Germany). Agarose gel electrophoresis and Qubit3.0 DNA detection (Qubit® dsDNA HS Assay Kit, Life Technologies, U.S.) were used to check the quality and quantity of the DNA after extraction. The amplification of the 16S rRNA gene (V3-V4 region) was performed and followed by high throughput sequencing using the MiSeq Illumina platform (Base-Clear, Leiden, the Netherlands). The primers used were 341F (5′−CCTACGGGNGGCWGCAG-3′) and 785R (5′-GACTACHVGGG-TATCTAATCC-3′). The analysis of the sequencing data was made by using the QIIME pipeline (version 1.9.0) (Caporaso et al., 2010), the demultiplexing and quality filtering was performed with Q = 20, r = 3, and p = 0.75 parameters. Chimeric sequences were removed using the UCHIME2 (version 9.0) algorithm (Edgar, 2016). Sequences were clustered into operational taxonomic units (OTUs) with a 97% similarity as a cutoff, with UCLUST algorithm (Edgar, 2010). Singletons were removed and OTUs with an occurrence less than three times in at least one sample were excluded. Taxonomic assignation was performed using the green genes database (gg_13_8) (McDonald et al., 2012) with UCLUST. Beta diversity workflows were used to generate microbial community composition and PCoA plots with the phyloseq and ggplot2 packages in the R environment. The statistical significance was tested with the ADONIS test. The differential abundances of OTUs among the mesophilic and thermophilic conditions was tested with the edgeR package (Robinson et al., 2010) with an adjusted p-value (FDR) cutoff of 0.001; the result is shown in a log to fold change plot. OTUs with significant differential abundances towards the thermophilic condition were analyzed with BLAST against the refseq_rna database to identify the closest related species. The four best hits were determined to build a phylogenetic tree. The sequences alignment was built with MUSCLE software (Edgar, 2004), and the alignment was trimmed with Gblocks (Castresana, 2000) in the Seaview alignment viewer (Gouy et al., 2010). The phylogenetic analysis was performed with the PhyML 3.0 software (Guindon et al., 2010), using the GTR + G + I + F substitution model with 200 bootstraps, the tree was drawn in FigTree (http://tree.bio.ed.ac.uk/software/figtree/). Raw sequences' data have been deposited in the NCBI SRA under accession number SRP110336.

3. Results and discussion

3.1. Effect of temperature shifts on AnMBR performance

High COD and phenol removal efficiencies were achieved up to 45 °C after two consecutive temperature shifts of the mesophilic AnMBR (Fig. 1. A). Under stable reactor operation during days 120—178 and at an OLR of 4.35 $gCOD \cdot L^{-1} \cdot d^{-1}$, the effluent COD was in the range of 0.1—2.54 $gCOD \cdot L^{-1}$ and the COD removal efficiencies were about 99.8%—93.7%. The increase in temperature from mesophilic (35 °C) to hypermesophilic (45 °C) conditions induced a decrease in the COD removal rate of the AnMBR from 0.26 ± 0.02 to 0.19 ± 0.01 $gCOD \cdot gVSS^{-1} \cdot d^{-1}$. A similar deterioration trend for phenol degradation was observed (Fig. 1B). The phenol conversion rate was about 3.16 ± 0.08 $mgPh \cdot gVSS^{-1} \cdot d^{-1}$ at 35 °C and 3.06 $mgPh \cdot gVSS^{-1} \cdot d^{-1}$ at 40 °C, decreasing to 2.10 ± 0.49 $mgPh \cdot gVSS^{-1} \cdot d^{-1}$ at 45 °C. The COD removal and phenol conversion rates (Table 1.) further decreased at 50 °C to 0.15 ± 0.02 $gCOD \cdot gVSS^{-1} \cdot d^{-1}$ and 1.63 ± 0.20 $mgPh \cdot gVSS^{-1} \cdot d^{-1}$, respectively. The phenol removal efficiency was in the range of 61.3—72.7%. After the temperature was shifted to 55 °C, the phenol conversion rate remained at about 1.42 ± 0.77 $mgPh \cdot gVSS^{-1} \cdot d^{-1}$, and a COD removal rate of 0.05 ± 0.02 $gCOD \cdot gVSS^{-1} \cdot d^{-1}$ was observed in the reactor. In contrast to COD to methane conversion, a more stable phenol conversion along the temperature shifts indicated a lower temperature susceptibility of the phenol degrading process compared to methanogenesis. Apparently, the biomass conversion capacity was disrupted by the temperature shift to thermophilic conditions (50 °C −55 °C) in combination with the high sodium concentration exposure (16 $gNa^+ \cdot L^{-1}$). Thus, OLR was decreased to 1.86 $gCOD \cdot L^{-1} \cdot d^{-1}$ to avoid system overloading. Hereafter, on days 227—240 the phenol removal efficiency improved to 76%, while the phenol conversion rate increased to 1.69 $mgPh \cdot gVSS^{-1} \cdot d^{-1}$. Phenol conversion rates at 55 °C were lower than observed at 35 °C, and a phenol removal efficiency of about 50% was achieved at the end of the experiment. Similarly, batch studies performed by Levén and Schnürer (2005, 2010) showed higher phenol conversion rates under mesophilic conditions compared to thermophilic conditions. This possibly can be ascribed to the enzymes involved in the degradation of phenol to benzoate, which are temperature sensitive above 48 °C, disturbing the phenol degradation at higher temperatures (Levén and Schnürer, 2005). The latter corresponds to the reduction in phenol conversion rates once the temperature was raised above hypermesophilic condition to 50 °C (Table 1.). Another possible explanation is the low microbial diversity of both Archaea and bacteria under thermophilic conditions (Levén et al., 2007).

The SMA increased about 23% at a temperature of 40 °C in comparison with 35 °C (0.26 ± 0.02 $gCOD-CH_4gVSS^{-1} \cdot d^{-1}$) (Table 2.). At 45 °C, a lower value than at 35 °C was found in agreement with the observed decrease in COD removal efficiency in the reactor. A minimum value of 0.04 ± 0.01 $gCOD-CH_4gVSS^{-1} \cdot d^{-1}$ was observed at 55 °C which is in line with the poor COD removal observed in the AnMBR right after the shift to this temperature. Furthermore, a similar decrease was observed by Fang et al. (2006)

who reported SMA values in UASB reactors treating phenolic wastewater of about 0.24 $gCOD-CH_4gVSS^{-1} \cdot d^{-1}$ and 0.09 $gCOD-CH_4gVSS^{-1} \cdot d^{-1}$ at 37 °C and 55 °C, respectively. The overall reactor biogas production decreased when temperature increased from 35 °C to 55 °C, as shown in Figure S1. However, the methane production rate did not recover after 50 days of operation at 55 °C in accordance with a low COD removal efficiency of 38%. Likewise, Kim and Lee (2016) pointed out that a temperature change between 45 °C and 50 °C had a critical impact on the methanogenic activity due to a severe restructuring of the reactor's microbial community, particularly of methanogens. A complete shift in the methanogenic subpopulations was also found in previous research, shifting a mesophilic UASB reactor to hyper-mesophilic and thermophilic conditions (Macario et al., 1991; van Lier et al., 1992, 1993).

Furthermore, the biomass concentration of the AnMBR reactor rapidly dropped to 8.98 $gVSS \cdot L^{-1}$ and 13.6 $gTSS \cdot L^{-1}$ when 55 °C was reached. The VSS:TSS ratio decreased from 0.77 at 35 °C to 0.59 once the operation at 55 °C was stable on day 268 (see Table 2.).

The aforementioned results suggest that if an AnMBR reactor is operated under mesophilic conditions and becomes suddenly exposed to hyper-mesophilic or thermophilic conditions, the observed overall methane production rate is also an indicator for the preserved phenol bioconversion capacity. The temperature shifts caused disturbances to the overall mesophilic AnMBR performance due to its impact on the biomass properties, filtration performance and microbial population structure as explained in the following sections.

3.2. Biomass properties affected by temperature shifts

3.2.1. Extracellular polymeric substances (EPS) and soluble microbial products (SMP)

Polysaccharides (PS) and proteins (PN) are accepted as primary constituents of SMP and EPS (Lin et al., 2014). The total SMP concentration was about 16.1 $mg.gVSS^{-1}$ at a temperature of 35 °C. A notable increase was observed from 50.5 ± 0.5 $mg.gVSS^{-1}$ at 45 °C to a maximum of 135.1 ± 2.0 $mg.gVSS^{-1}$ with a soluble PN content of 113.0 ± 1.7 $mg.gVSS^{-1}$ at 55 °C (Table 3). The observed increase is in agreement with Visvanathan et al. (2007) who found that thermophilic condition induces higher SMP production. It is noteworthy that the soluble PN to PS ratio increased about ten times from mesophilic to thermophilic conditions. Exoenzymes in the biomass and cell lysis products that were likely caused by the temperature change might be responsible for the higher amount of PN compared to PS (Neyens et al., 2004). However, overall the EPS concentration from both the PN and PS increased, but not gradually towards the thermophilic condition in contrast to what other studies have shown (Lin et al., 2009; Al-Amri et al., 2010). The latter can be attributed to the fact that the exposure time of biomass to each of the imposed temperatures was different. At 55 °C a maximum total EPS was found of about 104.9 ± 1.1 $mg.gVSS^{-1}$ whereas it was 57.8 ± 0.3 $mg.gVSS^{-1}$ at 35 °C.

Likewise, the variation of the EPS fingerprint can be observed in the FT-IR spectra in Figure S2. The peak around 3220 cm^{-1} is

Table 1
Phenol conversion and COD removal rates at 16 $gNa^+ \cdot L^{-1}$ after the temperature shifts.

Temperature	Phenol conversion rate [mg Ph $gVSS^{-1}$ d^{-1}]	COD removal rate [g COD $gVSS^{-1}$ d^{-1}]
35 °C	3.16 ± 0.08	0.26 ± 0.02
40 °C	3.06 ± 0.10	0.25 ± 0.00
45 °C	2.10 ± 0.49	0.19 ± 0.00
50 °C	1.63 ± 0.20	0.15 ± 0.02
55 °C[a]	1.42 ± 0.77	0.05 ± 0.03

[a] Under thermophilic condition phenol conversion rate increased to 1.69 $mgPh.gVSS^{-1}.d^{-1}$.

Table 2
SMA during the temperatures shifts from mesophilic to thermophilic conditions.

Temperature	Days	SMA [gCOD-CH$_4$gVSS^{-1}·d^{-1}]	VSS [g·L^{-1}]	VSS:TSS ratio
35 °C	131	0.26 ± 0.02	16.63 ± 0.07	0.77
35 °C	151	0.29 ± 0.22	16.87 ± 1.18	0.78
40 °C	179	0.32 ± 0.00	22.10 ± 0.56	0.77
45 °C	184	0.17 ± 0.01	22.72 ± 0.49	0.64
50 °C	191	0.27 ± 0.00	27.76 ± 1.37	0.63
55 °C	214	0.04 ± 0.01	9.65 ± 5.30	0.60
55 °C	241	N.D	8.98 ± 0.21	0.66

* At 268 days the VSS concentration was 9.5 g L^{-1} and the VSS:TSS ratio was 0.59.

Table 3
SMP and EPS during the temperatures shifts from mesophilic to thermophilic conditions. PN: Proteins, PS: Polysaccharides.

Temperature °C (Day)	SMP-PN [mg·gVSS^{-1}]	SMP-PS [mg·gVSS^{-1}]	SMP PN:PS ratio	Total SMP [mg·gVSS^{-1}]	EPS-PN [mg·gVSS^{-1}]	EPS-PS [mg·gVSS^{-1}]	EPS PN:PS ratio	Total EPS [mg·gVSS^{-1}]
35 (134)	5.3 ± 0.1	10.7 ± 0.7	0.5	16.0 ± 0.6	67.1 ± 0.3	13.6 ± 1.1	5.0	80.7 ± 0.8
35 (152)	5.3 ± 0.0	10.8 ± 1.1	0.5	16.1 ± 1.1	49.3 ± 0.1	8.4 ± 0.1	5.8	57.8 ± 0.3
40 (178)	35.6 ± 0.1	11.6 ± 0.0	3.1	47.2 ± 0.1	34.3 ± 2.4	8.2 ± 0.9	4.0	42.5 ± 3.3
45 (185)	40.7 ± 0.0	9.8 ± 0.5	4.2	50.5 ± 0.5	68.7 ± 9.3	10.5 ± 1.3	7.4	77.9 ± 10.5
50 (192)	34.6 ± 0.1	10.9 ± 0.8	3.2	45.4 ± 0.8	75.1 ± 2.4	14.0 ± 0.8	5.4	89.1 ± 1.6
55 (215)	102.9 ± 0.2	18.6 ± 1.6	5.5	121.6 ± 1.3	92.2 ± 0.7	12.9 ± 0.4	7.3	104.9 ± 1.1
55 (241)	113.0 ± 1.7	22.1 ± 0.3	5.1	135.1 ± 2.0	35.8 ± 5.3	17.3 ± 1.6	2.1	53.1 ± 6.9

attributed to the O-H stretching of the alcohols from PS and phenol (Wang et al., 2009; Dereli et al., 2015a). The two peaks at 1640 cm^{-1} and 840 cm^{-1} are due to N-H, C-N, and C=O vibration and stretching, and N-H wagging which are characteristic of secondary PN structures (Gupta and Thakur, 2015). The presence of a peak at 1000 cm^{-1} is evident in all the spectra and is due to the =C-H bending and C-O stretching of the alkanes from the carbohydrates or carbohydrates like substances (Sajjad and Kim, 2015). The peaks at 1400 cm^{-1} and 1570 cm^{-1} are due to C-H bending of the alkanes and alkenes from PS. At higher temperatures, the intensity of the peaks increased, especially the region around 1500 cm^{-1} typical of PN. The latter is also in agreement with the observed higher EPS concentrations because at more elevated temperatures their production might also be stimulated as a mechanism of protection for microorganisms [41]. Overall, more content of microbial substances, especially PN, was observed at higher temperatures in the AnMBR.
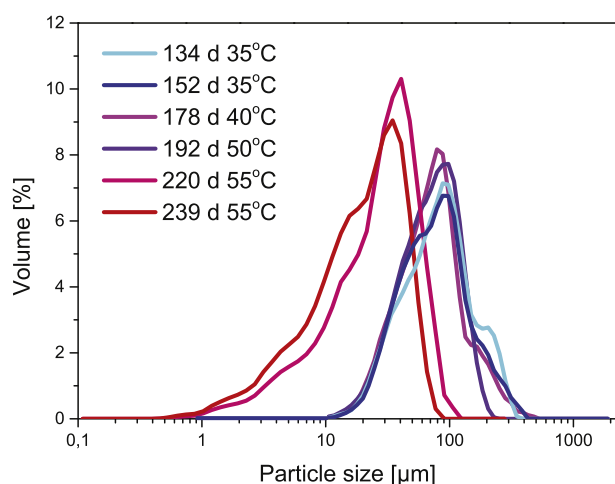

Fig. 2. Biomass particle size distribution at temperatures 35 °C, 40 °C, 50 °C and. 55 °C.

3.2.2. Particle size distribution

The median biomass particle size D50 was 89.4 μm at 35 °C on day 134 (Fig. 2). Along with the temperature increase to 40 °C and 50 °C, the median particle size decreased to 75.7 μm and 74.6 μm, on days 178 and 192, respectively. The gradual but fast increase from 45 °C to 55 °C caused biomass decay and floc breakage resulting in smaller particle size in the AnMBR as reported before by Gao et al. (2011). At thermophilic conditions, the median particle size D50 decreased to 22.4 μm and 21.0 μm on days 220 and 239, respectively. The mean particle size did not drop further until the end of the study. The observed decrease in biomass particle size of about 77% very likely contributed to the accumulation of fine particles leading to higher cake compactness. Increased cake layer compaction resulted in an increased transmembrane pressure (TMP) and membrane resistance at 55 °C.

3.3. Effect of temperature shifts on membrane filtration performance and biomass filterability

The mesophilic AnMBR exhibited a satisfactory filtration performance with TMP lower than 250 mbar between mesophilic and hypermesophilic conditions (Fig. 3 A.). The stable filtration performance was attributed to the operation far below the critical flux which was determined to be 26.0 L m^2·h^{-1} following the methods explained by Jeison and van Lier (2007). However, the TMP was negatively affected by the temperature shift to 55 °C and increased between 200 and 240 days to a maximum of 785 mbar. During this period, the membrane resistance was as high as 5.18 × 10^{13} m^{-1}. The appearance of small biomass particles and high protein concentration seemed to have a remarkable influence on the cake layer compaction that affected the filtration performance. The critical flux measured after reaching 55 °C was about 6.8 L m^2·h^{-1} indicating that the increased temperature resulted in a 74% decrease in the critical flux. Because the operational flux was close to the critical flux impacting the filtration performance negatively, a flux reduction was applied on day 218 resulting in a decrease in TMP and membrane resistance. The latter confirms that cake consolidation and compaction was the main explanation for the TMP and overall membrane resistance increase. Similarly, Jeison and van Lier (2008) showed that thermophilic operation (55 °C) causes a
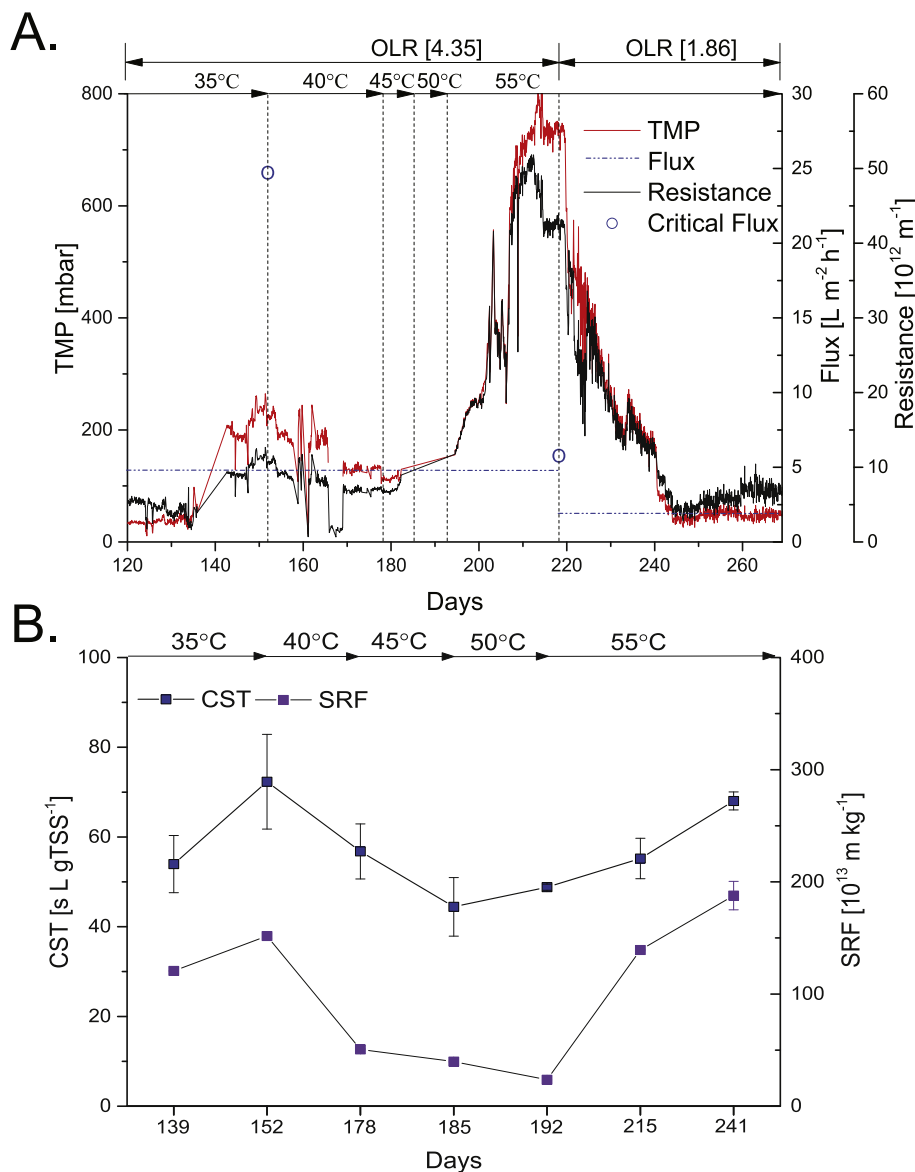
Fig. 3. A. TMP, membrane filtration resistance, and flux in the AnMBR. B. Biomass filterability: SRF, and CST at different operational temperatures.

significant decrease in the biomass particle size in a submerged AnMBR and consequently a fast reduction in critical flux from 20 to 6–7 L m²·h⁻¹.

As cake layer formation is the most significant fouling mechanism in the AnMBR, the specific resistance to filtration (SRF) may also refer to the quality of the cake accumulated on the membrane surface and therefore was also determined as an indication (Dereli et al., 2014). The SRF decreased from $151.7 \pm 2.2 \ 10^{13}$ m kg⁻¹ at 35 °C to $39.8 \pm 0.4 \ 10^{13}$ m kg⁻¹ at 45 °C and $23.6 \pm 0.3 \ 10^{13}$ m kg⁻¹ at 50 °C (Fig. 3 B). This decrease is attributed to the disruption of biomass flocs between 35 °C and 50 °C leading to smaller particle sizes, a less porous, more compact cake layer, and consequently lower SRF values. A decrease of SRF is in agreement with the observed biomass particle size reduction and soluble protein concentration increase (Lin et al., 2011). Correspondingly, the normalized capillary suction time (CST) values followed a similar trend than SRF. The CST ranged from 72.3 ± 10.5 s·L·gTSS⁻¹ at 35 °C to 44.4 ± 6.5 s·L·gTSS⁻¹ at 45 °C. At thermophilic conditions, the SRF increased to $187.8 \pm 12.7 \ 10^{13}$ m kg⁻¹, concomitantly the CST increased to

68.0 ± 2.0 s·L·gTSS⁻¹ on day 241. The increased SRF values indicated a cake layer with less compactness once the microbial decay products, SMP, and solids concentrations were steadied at 55 °C. It can be concluded from these results that the shifts above hyper-mesophilic conditions (45 °C) deteriorated the biomass filterability and could increase the fouling potential causing the observed detriment of membrane filtration performance.

3.4. Microbial community structure dynamics

Microbial community structure dynamics as a response to the temperature changes of the reactor biomass was analyzed by next-generation sequencing targeting the 16S rRNA gene. The principal coordinates' analysis indicated that the microbial community in the AnMBR experienced significant changes due to the consecutive shifts from mesophilic to hypermesophilic, and thermophilic conditions (Figure S3.A). Furthermore, ADONIS statistical test (Table 4) demonstrated significant differences ($p < 0.005$) of the microbial community along the temperature change ($R^2 = 0.31$). At the

Factor	R^2	Pr (>F)
Temperature [°C]	0.31	0.0019
Phenol specific loading rate [mgPh·gVSS^{-1}·d^{-1}]	0.21	0.009
COD specific loading rate [gCOD·gVSS^{-1}·d^{-1}]	0.14	0.1249

phylum level (Fig. 4. A), Firmicutes (41.08%), Euryarchaeota (32.00%), OP9 (6.50%), Chloroflexi (4.66%), Proteobacteria (4.42%) and Synergistetes (3.09%) were the dominant microorganisms after the long-term operation at 35 °C. Firmicutes, Proteobacteria and Chloroflexi, were recently reported as main phyla in anaerobic re-actors treating phenolic wastewater (Na et al., 2016; Wang et al., 2017b). In this study, all Firmicutes fell within the Clostridia class (Fig. 4B), the majority of these Clostridia belonged to the *Clostridium* genus (26.83%) (Fig. 4C). Putative phenol degraders under low phenol concentrations in AnSBRs are Clostridia-like (Rosenkranz et al., 2013). Chloroflexi were classified into the Anaerolineae class. Rosenkranz et al. (2013) also indicated that Anaerolineae has the highest proportion in mesophilic AnSBRs treating phenol. Methanomicrobia were mostly all assigned to the *Methanosaeta* genus (20.15%), and Methanobacteria (11.54%) were all assigned to the *Methanobacterium* genus. At 40 °C, the Proteo-bacteria phylum decreased significantly, and both Gammaproteo-bacteria and Deltaproteobacteria were affected. Interestingly, Wang et al. (2017b) indicated that the decrease in relative abundance of Proteobacteria, and Chloroflexi was observed with a reduction in

mesophilic phenol conversion. At 45 °C, the predominant phyla were shifted. The abundance of Methanomicrobia (*Methanosaeta* 28.89%) increased, and Firmicutes (28.27%) decreased significantly. At this temperature, a higher variation in the relative abundance in the AnMBR from the main phyla was observed concomitantly with the decrease in phenol conversion rate of the reactor. Once the temperature rose to 50 °C, the increase in relative abundance of the genus *Kosmotoga* was remarkable, which is known to grow over a wide high-temperature range and tolerate highly saline conditions. At 55 °C the predominant phyla were similar as at 35 °C except for Thermotogae that increased significantly from 0.45% at 35 °C to 6.36% at 55 °C. Overall, the relative abundance of methanogens was stable, and in the case of OP9, Synergistetes and Thermotogae increased. Recently, Synergistetes was suggested by Poirier et al. (2016) as an early warning indicator of phenol inhibition towards anaerobic microbiota. On the contrary, the abundance of Firmicutes and Proteobacteria decreased. Specifically, microorganisms from these two phyla have been reported to have the capacity of syn-trophically degrading aromatic compounds including phenol, such as the genera *Syntrophorhabdus* and *Pelotomaculum* (Chen et al., 2008; Nobu et al., 2015). A syntrophic association between phenol carboxylating, benzoate degrading and hydrogenotrophic methane-producing microorganisms is required for the complete phenol degradation to methane. There was no evidence of having *Syntrophorhabdus* in the biomass, as was recently observed at high salinity under mesophilic conditions (Wang et al., 2017b), but there were OTUs with high similarity to *Pelotomaculum* at thermophilic conditions. Moreover, a decrease in abundance of *Meth-anobacterium* was observed while the reactor performance
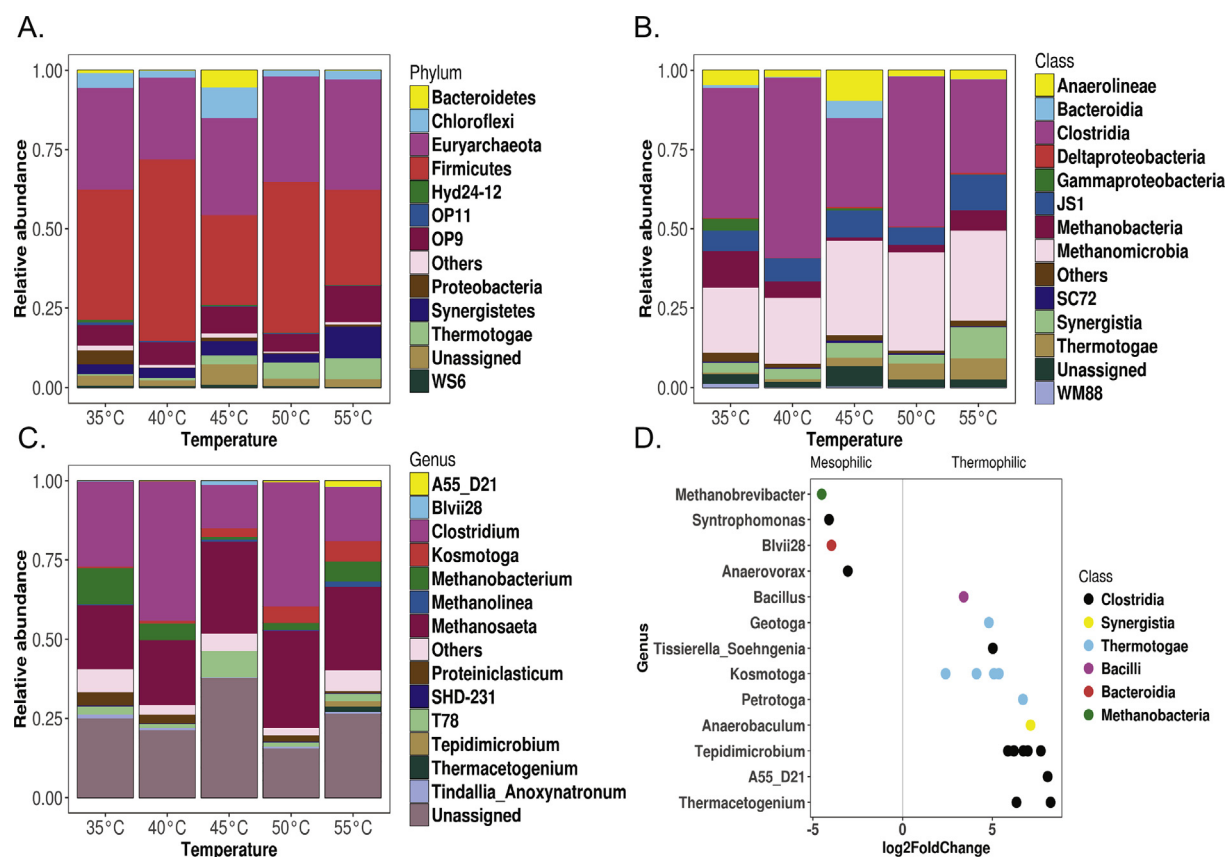

Fig. 4. Analysis of microbial community structure dynamics due to operational temperature. A. OTUs relative abundance at the phylum level. B. OTUs relative abundance at the class level. C. OTUs relative abundance at the genus level. D. Log2fold change plot for the differential abundance of the OTUs among the mesophilic and thermophilic conditions at (p-value < 0.001).
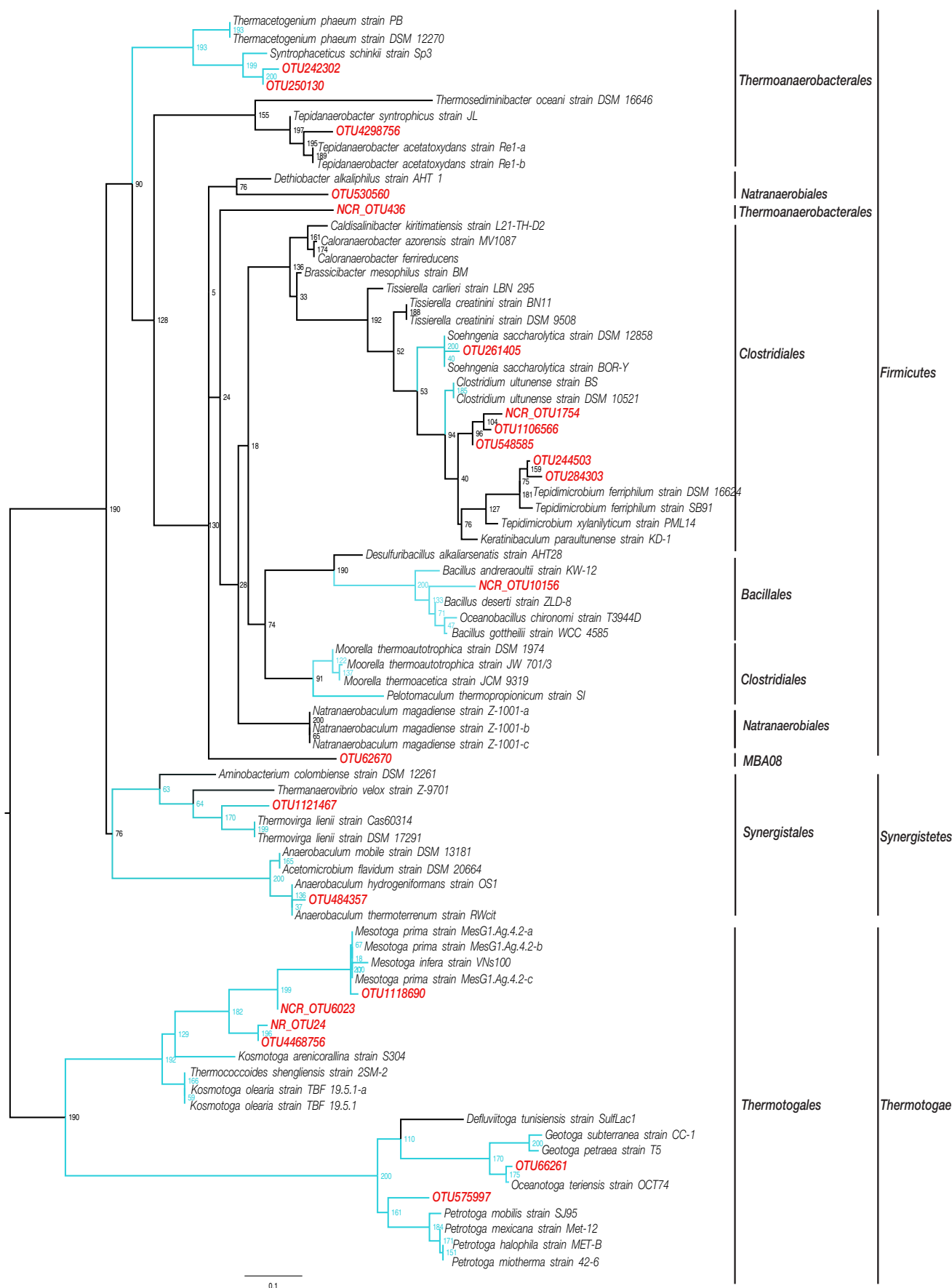
Fig. 5. Phylogenetic tree of OTUs with significant differential abundances towards thermophilic (55 °C) phenol degradation. 0.1 horizontal scale shows the length of the branch that represents a genetic change of 0.1. In red: 21 identified OTUs. In light blue: clades with 11 OTUs close to species reported in the process of phenol and similar aromatic compounds degradation. (For interpretation of the references to color in this figure legend, the reader is referred to the Web version of this article.)

decreased, indicating the importance of an H_2-scavenging methanogen partner in syntrophic association with phenol degraders (Qiu et al., 2008).

The differential abundances of the OTUs between mesophilic and thermophilic conditions were calculated and described in a $\log_2$ fold change plot at class and genus level (Fig. 4D). 21 OTUs that have differential abundance were identified. The genera *Methanobrevibacter*, *Syntrophomonas*, *Blivii28*, and *Anerovorax*, were up to 9 times higher in abundance at mesophilic than compared to thermophilic conditions. Conversely, the genera *Thermoacetogenium*, *A55_D21*, *Tepidimicrobium*, *Anaerobaculum*, and *Petrotoga* increased in a range from 12 to 16 times under thermophilic conditions. The abundance of these OTUs is shown in Figure S3.B. From these OTUs, a phylogenetic tree was built with the four best hits of each (Fig. 5.). The analysis grouped 11 OTUs within clades with species that have been reported in phenolic wastewater treatment reactors, oil production sites, terephthalic acid, and coking wastewater treatment processes (see Table S1.).

The phylogenetic distribution of the microbial community and functionality was affected by the temperature increase in the AnMBR. However, it is still unclear whether operating the reactor under hypermesophilic (40 °C—45 °C) or thermophilic conditions would maximize the phenol conversion rate and corresponding microbial syntrophic associations. This is the first time that an AnMBR has been used to explore the degradation of phenol at high temperature and high salinity. Further research is needed to account the long-term effects of thermophilic operation on the phenol bioconversion rate to identify whether it increases to the same or higher levels than under mesophilic conditions. Also, long-term adaptation at 55 °C could further reveal the differences in microbial population structure with similar functionality in comparison to the operation at 35 °C. Based on the overall effects of the shifts from mesophilic to hyper-mesophilic and subsequent thermophilic operation, this study suggests that highly saline phenolic wastewaters are attainable to be treated in a mesophilic AnMBR within the hyper-mesophilic temperature range without the need of long-term acclimation. Although the exact temperature span of the species involved are not known and net growth yields will drop to a minimum reaching the limits of the growth temperature, operation at hypermesophilic conditions e.g. 42-45 °C will bring operational energy benefits when treating high-temperature wastewaters, especially when opting for process water reuse.

4. Conclusions

This study was undertaken to evaluate the temperature susceptibility of the phenol bioconversion capacity over a range of 35 °C to 55 °C in an AnMBR at high salinity conditions. Due to the temperature shifts over a range of 35 °C to 55 °C in an AnMBR operated at 16 gNa$^+$·L^{-1}, the COD removal and phenol conversion rates decreased from 0.26 gCOD·gVSS^{-1}·d^{-1} to 0.075 gCOD·gVSS^{-1}·d^{-1}, and 3.16 mgPh·gVSS^{-1}·d^{-1} to 1.69 mgPh·gVSS^{-1}·d^{-1}, respectively. Results clearly showed that the phenol degradation process was less susceptible for the temperature shifts than methanogenesis. The membrane filtration performance was negatively affected by the temperature increases coinciding with a 77% particle size decrease and a higher content of microbial protein-like substances. Microbial community abundance of known phyla for syntrophic phenol degradation decreased as the temperature was shifted. Twenty-one OTUs were identified with differential abundance between mesophilic and thermophilic operation, and eleven of them were similar to species reported in aromatic degradation processes. These findings suggest that under mesophilic and hyper-mesophilic conditions, the phenol degradation capacity of the AnMBR at high salinity was more stable compared to thermophilic conditions. Therefore, by controlling the temperature at the lower limit of the hyper-mesophilic range, operation at e.g. 42-45 °C will bring operational energy benefits when treating high-temperature wastewaters opting for water reuse. Therefore, and considering that the phenol conversion capacity is preserved, it is certainly worthwhile to further explore the treatment potentials at the hyper-mesophilic temperature range.

Appendix A. Supplementary data

Supplementary data related to this article can be found at https://doi.org/10.1016/j.chemosphere.2018.09.023.

References

Al-Amri, A., Salim, M.R., Aris, A., 2010. The effect of different temperatures and fluxes on the performance of membrane bioreactor treating synthetic-municipal wastewater. Desalination 259, 111—119.

Boušková, A., Dohányos, M., Schmidt, J.E., Angelidaki, I., 2005. Strategies for changing temperature from mesophilic to thermophilic conditions in anaerobic CSTR reactors treating sewage sludge. Water Res. 39, 1481—1488.

Caporaso, J.G., Kuczynski, J., Stombaugh, J., Bittinger, K., Bushman, F.D., Costello, E.K., Fierer, N., Pena, A.G., Goodrich, J.K., Gordon, J.I., Huttley, G.A., Kelley, S.T., Knights, D., Koenig, J.E., Ley, R.E., Lozupone, C.A., McDonald, D., Muegge, B.D., Pirrung, M., Reeder, J., Sevinsky, J.R., Turnbaugh, P.J., Walters, W.A., Widmann, J., Yatsunenko, T., Zaneveld, J., Knight, R., 2010. QIIME allows analysis of high-throughput community sequencing data. Nat. Methods 7, 335—336.

Castresana, J., 2000. Selection of conserved blocks from multiple alignments for their use in phylogenetic analysis. Mol. Biol. Evol. 17, 540—552.

Chen, C.L., Wu, J.H., Liu, W.T., 2008. Identification of important microbial populations in the mesophilic and thermophilic phenol-degrading methanogenic consortia. Water Res. 42, 1963—1976.

De Amorim, E.L.C., Sader, L.T., Silva, E.L., 2015. Effects of the organic-loading rate on the performance of an anaerobic fluidized-bed reactor treating synthetic wastewater containing phenol. J. Environ. Eng. 141.

Dereli, R.K., Ersahin, M.E., Ozgun, H., Ozturk, I., Jeison, D., van der Zee, F., van Lier, J.B., 2012. Potentials of anaerobic membrane bioreactors to overcome treatment limitations induced by industrial wastewaters. Bioresour. Technol. 122, 160—170.

Dereli, R.K., Grelot, A., Heffernan, B., van der Zee, F.P., van Lier, J.B., 2014. Implications of changes in solids retention time on long term evolution of sludge filterability in anaerobic membrane bioreactors treating high strength industrial wastewater. Water Res. 59, 11—22.

Dereli, R.K., Heffernan, B., Grelot, A., Van Der Zee, F.P., Van Lier, J.B., 2015a. Influence of high lipid containing wastewater on filtration performance and fouling in AnMBRs operated at different solids retention times. Separ. Purif. Technol. 139, 43—52.

Dereli, R.K., Loverdou, L., van der Zee, F.P., van Lier, J.B., 2015b. A systematic study on the effect of substrate acidification degree and acidogenic biomass on sludge filterability. Water Res. 82, 94—103.

Dubois, M., Gilles, K.A., Hamilton, J.K., Rebers, P.A., Smith, F., 1956. Colorimetric method for determination of sugars and related substances. Anal. Chem. 28, 350—356.

Duncan, J., Bokhary, A., Fatehi, P., Kong, F., Lin, H., Liao, B., 2017. Thermophilic membrane bioreactors: a review. Bioresour. Technol. 243, 1180—1193.

Edgar, R., 2016. UCHIME2: Improved Chimera Prediction for Amplicon Sequencing. bioRxiv.

Edgar, R.C., 2004. MUSCLE: a multiple sequence alignment method with reduced time and space complexity. BMC Bioinf. 5.

Edgar, R.C., 2010. Search and clustering orders of magnitude faster than BLAST. Bioinformatics 26, 2460—2461.

Fang, H.H.P., Liang, D.W., Zhang, T., Liu, Y., 2006. Anaerobic treatment of phenol in wastewater under thermophilic condition. Water Res. 40, 427—434.

Frølund, B., Palmgren, R., Keiding, K., Nielsen, P.H., 1996. Extraction of extracellular polymers from activated sludge using a cation exchange resin. Water Res. 30, 1749—1758.

Gao, W.J., Leung, K.T., Qin, W.S., Liao, B.Q., 2011. Effects of temperature and temperature shock on the performance and microbial community structure of a submerged anaerobic membrane bioreactor. Bioresour. Technol. 102, 8733—8740.

Gouy, M., Guindon, S., Gascuel, O., 2010. Sea view version 4: a multiplatform graphical user interface for sequence alignment and phylogenetic tree building. Mol. Biol. Evol. 27, 221–224.

Guindon, S., Dufayard, J.F., Lefort, V., Anisimova, M., Hordijk, W., Gascuel, O., 2010. New algorithms and methods to estimate maximum-likelihood phylogenies: assessing the performance of PhyML 3.0. Syst. Biol. 59, 307–321.

Gupta, A., Thakur, I.S., 2015. Study of optimization of wastewater contaminant removal along with extracellular polymeric substances (EPS) production by a thermotolerant Bacillus sp. ISTVK1 isolated from heat shocked sewage sludge. Bioresour. Technol. 213, 21–30.

Jeison, D., van Lier, J.B., 2007. Thermophilic treatment of acidified and partially acidified wastewater using an anaerobic submerged MBR: factors affecting long-term operational flux. Water Res. 41, 3868–3879.

Jeison, D., van Lier, J.B., 2008. Feasibility of thermophilic anaerobic submerged membrane bioreactors (AnSMBR) for wastewater treatment. Desalination 231, 227–235.

Kim, J., Lee, C., 2016. Response of a continuous anaerobic digester to temperature transitions: a critical range for restructuring the microbial community structure and function. Water Res. 89, 241–251.

Levén, L., Eriksson, A.R.B., Schnürer, A., 2007. Effect of process temperature on bacterial and archaeal communities in two methanogenic bioreactors treating organic household waste. FEMS Microbiol. Ecol. 59, 683–693.

Levén, L., Nyberg, K., Schnürer, A., 2012. Conversion of phenols during anaerobic digestion of organic solid waste — a review of important microorganisms and impact of temperature. J. Environ. Manag. 95 (Suppl. ment), S99–S103.

Levén, L., Schnürer, A., 2005. Effects of temperature on biological degradation of phenols, benzoates and phthalates under methanogenic conditions. Int. Biodeterior. Biodegrad. 55, 153–160.

Levén, L., Schnürer, A., 2010. Molecular characterisation of two anaerobic phenol-degrading enrichment cultures. Int. Biodeterior. Biodegrad. 64, 427–433.

Lin, H., Liao, B.-Q., Chen, J., Gao, W., Wang, L., Wang, F., Lu, X., 2011. New insights into membrane fouling in a submerged anaerobic membrane bioreactor based on characterization of cake sludge and bulk sludge. Bioresour. Technol. 102, 2373–2379.

Lin, H., Peng, W., Zhang, M., Chen, J., Hong, H., Zhang, Y., 2013. A review on anaerobic membrane bioreactors: applications, membrane fouling and future perspectives. Desalination 314, 169–188.

Lin, H., Zhang, M., Wang, F., Meng, F., Liao, B.Q., Hong, H., Chen, J., Gao, W., 2014. A critical review of extracellular polymeric substances (EPSs) in membrane bioreactors: characteristics, roles in membrane fouling and control strategies. J. Membr. Sci. 460, 110–125.

Lin, H.J., Xie, K., Mahendran, B., Bagley, D.M., Leung, K.T., Liss, S.N., Liao, B.Q., 2009. Sludge properties and their effects on membrane fouling in submerged anaerobic membrane bioreactors (SAnMBRs). Water Res. 43, 3827–3837.

Macario, A.J.L., Visser, F.A., Van Lier, J.B., De Macario, E.C., 1991. Topography of methanogenic subpopulations in a microbial consortium adapting to thermophilic conditions. J. Gen. Microbiol. 137, 2179–2189.

McDonald, D., Price, M.N., Goodrich, J., Nawrocki, E.P., Desantis, T.Z., Probst, A., Andersen, G.L., Knight, R., Hugenholtz, P., 2012. An improved Greengenes taxonomy with explicit ranks for ecological and evolutionary analyses of bacteria and archaea. ISME J. 6, 610–618.

Muñoz Sierra, J.D., Lafita, C., Gabaldón, C., Spanjers, H., van Lier, J.B., 2017. Trace metals supplementation in anaerobic membrane bioreactors treating highly saline phenolic wastewater. Bioresour. Technol. 234, 106–114.

Muñoz Sierra, J.D., Oosterkamp, M.J., Wang, W., Spanjers, H., van Lier, J.B., 2018. Impact of long-term salinity exposure in anaerobic membrane bioreactors treating phenolic wastewater: performance robustness and endured microbial community. Water Res. 141, 172–184.

Na, J.G., Lee, M.K., Yun, Y.M., Moon, C., Kim, M.S., Kim, D.H., 2016. Microbial community analysis of anaerobic granules in phenol-degrading UASB by next generation sequencing. Biochem. Eng. J. 112, 241–248.

Neyens, E., Baeyens, J., Dewil, R., De Heyder, B., 2004. Advanced sludge treatment affects extracellular polymeric substances to improve activated sludge dewatering. J. Hazard Mater. 106, 83–92.

Nobu, M.K., Narihiro, T., Hideyuki, T., Qiu, Y.-L., Sekiguchi, Y., Woyke, T., Goodwin, L., Davenport, K.W., Kamagata, Y., Liu, W.-T., 2015. The genome of Syntrophorhabdus aromaticivorans strain UI provides new insights for syntrophic aromatic compound metabolism and electron flow. Environ. Microbiol. 17, 4861–4872.

Poirier, S., Bize, A., Bureau, C., Bouchez, T., Chapleur, O., 2016. Community shifts within anaerobic digestion microbiota facing phenol inhibition: towards early warning microbial indicators? Water Res. 100, 296–305.

Qiu, Y.L., Hanada, S., Ohashi, A., Harada, H., Kamagata, Y., Sekiguchi, Y., 2008. Syntrophorhabdus aromaticivorans gen. nov., sp. nov., the first cultured anaerobe capable of degrading phenol to acetate in obligate syntrophic associations with a hydrogenotrophic methanogen. Appl. Environ. Microbiol. 74, 2051–2058.

Ramakrishnan, A., Gupta, S.K., 2006. Anaerobic biogranulation in a hybrid reactor treating phenolic waste. J. Hazard Mater. 137, 1488–1495.

Ramakrishnan, A., Surampalli, R.Y., 2013. Performance and energy economics of mesophilic and thermophilic digestion in anaerobic hybrid reactor treating coal wastewater. Bioresour. Technol. 127, 9–17.

Robinson, M.D., McCarthy, D.J., Smyth, G.K., 2010. edgeR: a Bioconductor package for differential expression analysis of digital gene expression data. Bioinformatics 26, 139–140.

Rosenkranz, F., Cabrol, L., Carballa, M., Donoso-Bravo, A., Cruz, L., Ruiz-Filippi, G., Chamy, R., Lema, J.M., 2013. Relationship between phenol degradation efficiency and microbial community structure in an anaerobic SBR. Water Res. 47, 6739–6749.

Sajjad, M., Kim, K.S., 2015. Studies on the interactions of Ca2+ and Mg2+ with EPS and their role in determining the physicochemical characteristics of granular sludges in SBR system. Process Biochem. 50, 966–972.

van Lier, J.B., Grolle, K.C.F., Stams, A.J.M., de Macario, E.C., Lettinga, G., 1992. Start-up of a thermophilic upflow anaerobic sludge bed (UASB) reactor with mesophilic granular sludge. Appl. Microbiol. Biotechnol. 37, 130–135.

van Lier, J.B., Hulsbeek, J., Stams, A.J.M., Lettinga, G., 1993. Temperature susceptibility of thermophilic methanogenic sludge: implications for reactor start-up and operation. Bioresour. Technol. 43, 227–235.

van Lier, J.B., van der Zee, F.P., Frijters, C.T.M.J., Ersahin, M.E., 2015. Celebrating 40 years anaerobic sludge bed reactors for industrial wastewater treatment. Rev. Environ. Sci. Biotechnol. 14, 681–702.

Visvanathan, C., Choudhary, M.K., Montalbo, M.T., Jegatheesan, V., 2007. Landfill leachate treatment using thermophilic membrane bioreactor. Desalination 204, 8–16.

Wang, W., Han, H., 2012. Recovery strategies for tackling the impact of phenolic compounds in a UASB reactor treating coal gasification wastewater. Bioresour. Technol. 103, 95–100.

Wang, W., Han, H., Yuan, M., Li, H., Fang, F., Wang, K., 2011a. Treatment of coal gasification wastewater by a two-continuous UASB system with step-feed for COD and phenols removal. Bioresour. Technol. 102, 5454–5460.

Wang, W., Ma, W., Han, H., Li, H., Yuan, M., 2011b. Thermophilic anaerobic digestion of Lurgi coal gasification wastewater in a UASB reactor. Bioresour. Technol. 102, 2441–2447.

Wang, W., Wang, S., Ren, X., Hu, Z., Yuan, S., 2017a. Rapid establishment of phenol- and quinoline-degrading consortia driven by the scoured cake layer in an anaerobic baffled ceramic membrane bioreactor. Environ. Sci. Pollut. Control Ser. 24, 26125–26135.

Wang, W., Wu, B., Pan, S., Yang, K., Hu, Z., Yuan, S., 2017b. Performance robustness of the UASB reactors treating saline phenolic wastewater and analysis of microbial community structure. J. Hazard Mater. 331, 21–27.

Wang, W., Yang, K., Muñoz Sierra, J., Zhang, X., Yuan, S., Hu, Z., 2017c. Potential impact of methyl isobutyl ketone (MIBK) on phenols degradation in an UASB reactor and its degradation properties. J. Hazard Mater. 333, 73–79.

Wang, Z., Wu, Z., Tang, S., 2009. Extracellular polymeric substances (EPS) properties and their effects on membrane fouling in a submerged membrane bioreactor. Water Res. 43, 2504–2512.